OPEN ACCESS

European Journal of Engineering Science and Technology
ISSN 2538-9181

Creation of a Laboratory Fog Chamber for Testing Optical Sensors

Wolfgang Mühleisen*[1], Cristina Consani[1], Povilas Smaliukas[1], Markus Bainschab[1], Georg Brunnhofer[2], Andreas Tortschanoff[1]

[1] SAL Silicon Austria Labs GmbH, Europastr.12, Austria
[2] AVL List GmbH, Hans-List-Platz 1, Austria

ARTICLE INFO

Keywords:
Fog Chamber, LIDAR Test Environment, Mist Maker, Ultrasonic Nebulizer

ABSTRACT

LIDAR sensors and systems are gaining popularity, but their effectiveness can be compromised by light reflections in foggy conditions. To address the need for small, laboratory-scale testing systems, a fog chamber was developed and tested to have a laboratory environment. Two different methods to produce fog were evaluated: hot steam and ultrasonic nebulizers. The cold fog from ultrasonic nebulizers was more prone to stratification, while the hot fog from hot steam produced rather disturbing condensation for the measurement. All this was solved by implementing improving aids such as a ventilation and windscreen wiper system. First to mitigate the fog stratification with help of circulation and second to prevent condensation with help of wiping the windows in the measurement path. Ultimately, the ultrasonic nebulizers showed their strengths in the experiment due to the lower influence of the enhancement aids on the signal quality, which is why they are recommended as a fog source.

1. Introduction

For the testing and application of systems such as LIDAR (Light Imaging, Detection and Ranging), meteorological test chambers are used which can simulate rain or fog (Linnhoff et al., 2022; Duthon et al., 2020; Kutila et al., 2018; Montalban et al., 2021). Such test chambers can usually be walked or driven through, and they are therefore very large and elaborately designed. Unlike radar technology, LIDAR technology does not use radio waves but visible or infrared (IR) light that is emitted in pulses and reflected by objects. The distance is calculated from the time it takes the light to travel the source-object distance and back. By means of many pulses in scanning mode, it is thus possible to create an image of contours (Hahner et al., 2021; Royo et al., 2019). Such sensor information forms the basis for the function of numerous driving and safety systems, which are intended to provide information and prevent accidents with appropriate warnings and vehicle interventions (Mothershed et al., 2020; Wu et al., 2018). However, light rays can be scattered or absorbed by rain, fog, snowfall or dust particles, limiting the range and accuracy of LIDAR-based object detection in outdoor scenarios. Access to meteorological test chambers can be very costly and require long waiting times. In order to advance the testing and optimization of LIDAR systems in adverse meteorological conditions,

* Corresponding Author's E-Mail Address: wolfgang.muehleisen@silicon-austria.com

Cite this article as:
Mühleisen, W., Consani, C., Smaliukas, P., Bainschab, M., Brunnhofer, G., Tortschanoff, A. (2024). Creation of a Laboratory Fog Chamber for Testing Optical Sensors. *European Journal of Engineering Science and Technology, 7*(2): 31-43. https://doi.org/10.33422/ejest.v7i2.1427

it is necessary to develop and provide affordable test environments on a laboratory scale (Ballesta-Garcia et al., 2021; Sawant et al., 2012; Singh et al., 2011).

Fog is understood as a water aerosol formed by fine water droplets floating in the air with droplet sizes in the micrometre range (Liu et al., 2020). Various methods can be used to artificially generate fog, e.g. with superheated steam, ultrasonic treatment or chemical fog fluid. The research objectives are the generation of a functional fog chamber with different fog densities for testing on optical sensors. The focus is on the application, characterization and analysis of two different fog sources to establish and answer hypotheses.

As we are interested in mimicking natural fog, chemical-based fog fluid was not considered here. Instead, we report on the experimental characterization of the fog-chamber operated with hot-steam fog and with cold ultrasonically generated fog. Particularly, we will discuss how the generation mechanism of the fog affects the fog properties (e.g., droplet size and temperature) and the performance of the chamber.

2. Methods

2.1. Fog Chamber Description

The fog chamber is made of black polyethylene (PE) material and measures 210 by 19 by 19 centimetres (Figure 1). It was built in such a way that experiments can be carried out with two different, separate fog sources, as described in section *2.2*. For the determination of the visibility, a laser beam passes through the closed fog chamber through an inlet and outlet glass pane and is detected on the other side using an optical power meter. The used detector and laser components are: A power meter reading device “Thorlabs PM400” (USB connection and recorder function) with a connected photodiode power sensor “Thorlabs S120C” (range 400 – 1100 nm, power range 50 nW – 50 mW, resolution 10 nW). The laser source is a “Thorlabs PL202” (class 2 compact laser module with USB connector, 635 nm, 0.9 mW, built-in electrical filter and photodiode feedback against power supply noise and constant light power output).

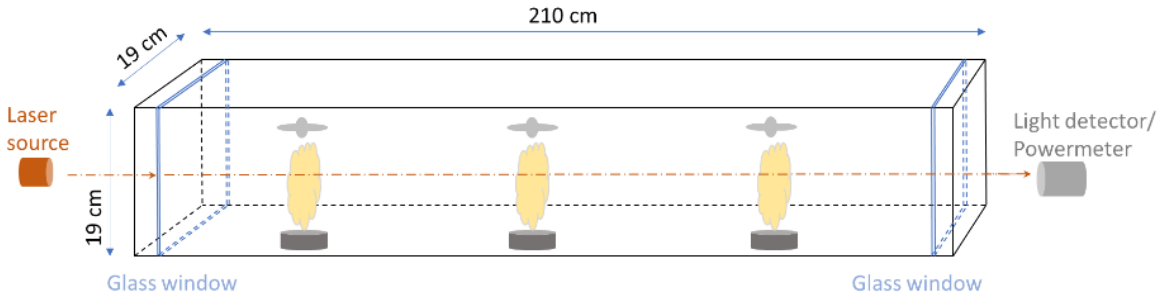

Figure 1. Sketch of the fog chamber with dimensions and setup idea

In addition, the chamber can be closed on the top side with a plastic lid (Figure 2a) or glass panes (Figure 2b). A top cover with transparent glass panes provides the advantage to have a better look into the inside of the fog chamber.

The fog chamber is designed to not be hermetically closed at this stage. This way, it is also possible to dynamically monitor the evolution of the fog in the system, from very dense to its dissipation. This feature is potentially attractive for rapidly testing the performance of LIDAR systems in different (and varying) visibility conditions.

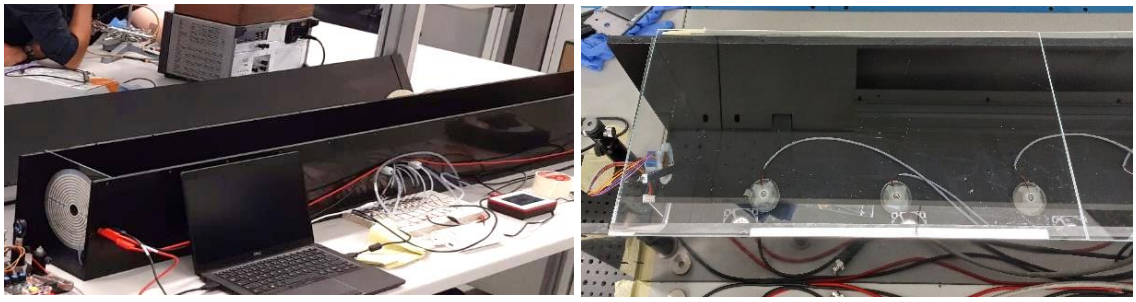

Figures 2a, 2b. Picture of the chamber with a plastic lid and glass panes option

2.2. Fog Generation

Two different methods of fog generation were investigated and tested for suitability in a fog chamber: generation of steam by means of a steam cleaner (1) and fog generation by means of piezo ultrasonic nebulisers (2).

(1) Fog source - steam cleaner

In the steam cleaner (Kärcher SC3, max. steam pressure 3.5 bar, 1900 W) water is vaporised in a pressure vessel and hot steam is created (Figures 3a, 3b).

Figures 3a, 3b. Steam cleaner as a fog generation source and inlet opening into the chamber

(2) Fog source - piezoelectric transducer

Another way to create fog is with help of a piezo transducer also called humidifier or mist maker. The used product (Seed water atomization, 5V, 2 W) consists of a perforated platelet, vibrating at a high frequency of 105 ± 5 kHz. The plate whips water into tiny droplets, which are sprayed as mist. In addition, an in-house developed 3D printed housing with DI-water reservoir was created to have a sprayer unit (Figure 4). To ensure the generation of a homogeneous fog throughout the chamber, 10 nebulizer sprayer units were mounted on the bottom side, every 17 cm along the entire length of the chamber.

Figure 4. Piezo transducer sprayer unit as a fog generation source

2.3. Strategy for Reducing/Avoiding Condensation in the Measurement Path and Preventing the Formation of Fog Layers

Condensation occurs when a lot of moisture accumulates on surfaces and the air is already saturated, causing the moisture to condense in the form of water droplets. Since such water droplets are located in the measuring path of the light beam and affect the optical signals, it is necessary to take precautions to prevent or reduce condensation in the best possible way.

To minimize the effect of condensation inside the chamber at the entrance window (laser source side) and at the exit window (detector side), a windscreen wiper was mounted on each window and tested. (Figures 5a, 5b).

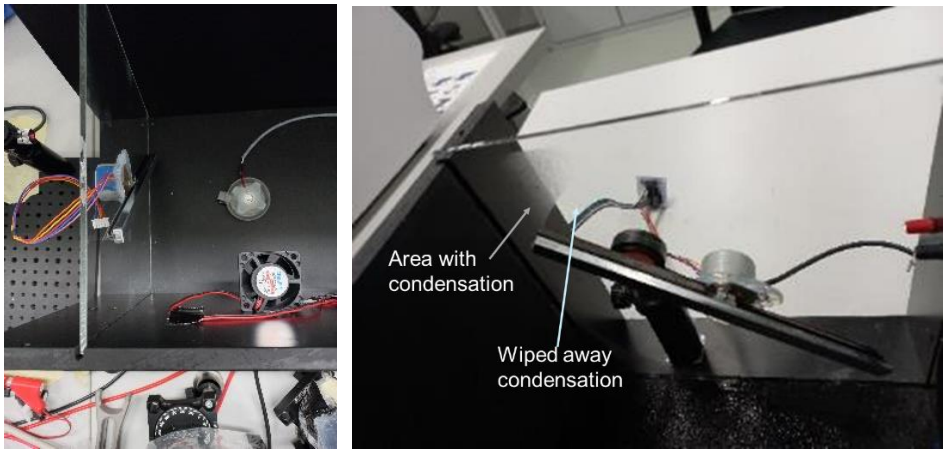

Figures 5a, 5b. Pictures of the entrance and outrance windows with a windscreen wiper on the inner windows side to minimize the influence of condensation on the optical signals.

To prevent fog stratification, which could cause artefacts on the optical signals, slow-running fans (Xindafan XD4020DC) were installed to introduce some air circulation (Figure 6). Running the 12 V fans at 3 V was sufficient to prevent stratification effects.

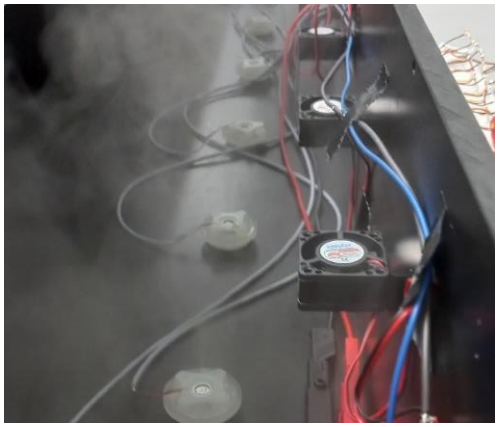

Figure 6. Picture of the added low-speed ventilation system

3. Testing and Characterization of the Individual Components

In this section, the equipment and chamber is tested, characterized and evaluated. In Figure 7, a functioning chamber is shown.

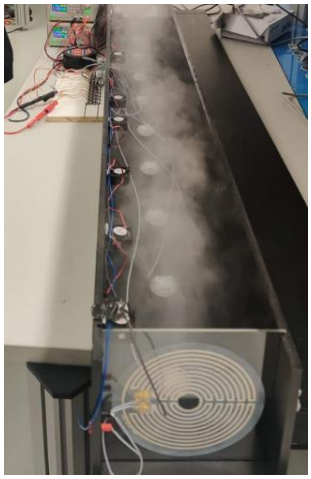

Figure 7. Picture of the open fog chamber with 10 sprayer units in series at a distance of 17 cm

3.1. Piezo Vibrating Element and Fog Characterization Using a Microscope

Due to the small design of the flat piezo nebulizers - diameter 2 cm (Figure 8a), it is possible to characterize them under the microscope (Figures 8b, 8c). For the vibrating element, small holes are visible with the microscope, and they are in the range between 4 and 6 µm which agrees with data from literature (Kooij et al., 2019). One highlight is that even the sprayed fog can be characterized under the microscope (Figure 8d), which allows a statement about the particle sizes (Figure 8e).

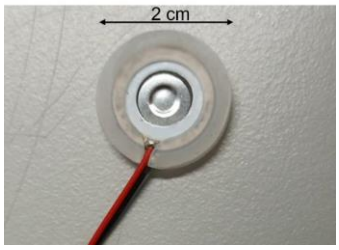

Figure 8a. Picture of the piezo vibrating element

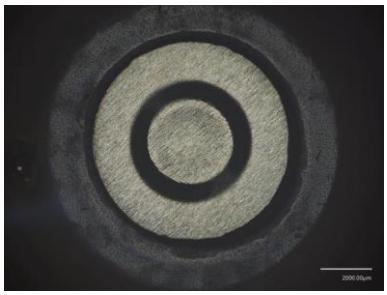

Figure 8b. Zoomed-in picture of the piezo vibrating element under microscope

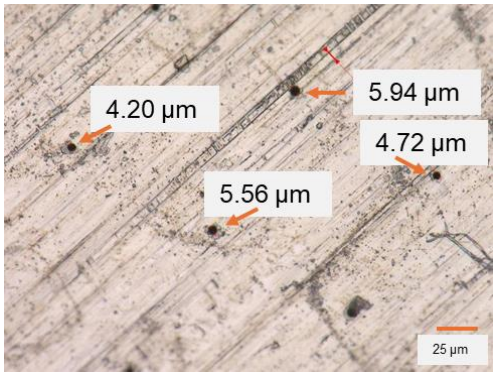

Figure 8c. Strong zoomed-in picture of the piezo vibrating element under microscope - showing holes

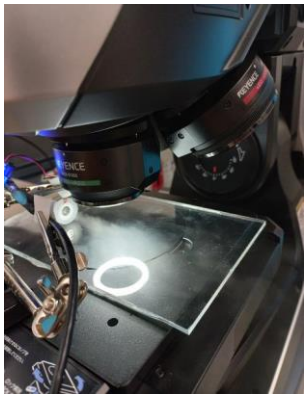

Figure 8d. Picture of the setup of the spraying piezo vibrating element under the microscope

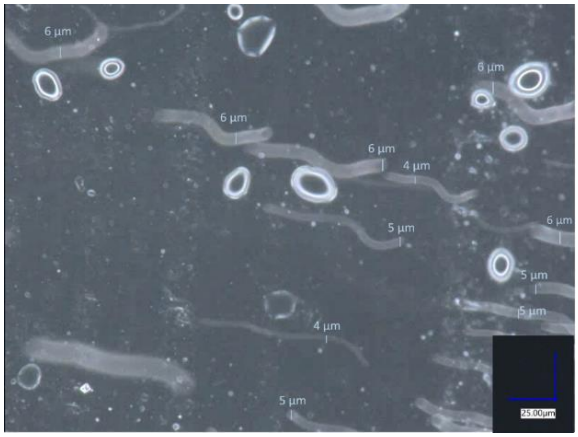

Figure 8e. Microscope picture of the flying by fog particles

By placing the vibrating piezoelectric element under the microscope, the generated water particles can be imaged in real time (Figure 8e). The large droplets in the picture are deposited on the glass window. A high-speed particle stream is emitted by the nebulizers. Such fast particles appear as lines in the image. A cross-section through the line provides an estimation of the particle diameter. Of course, only the size of particles which move within the focal plane can be retrieved correctly. Shown in a raincloud plot (Figure 8f), which was created from the measurement data of several individual microscope images, it becomes clear that an accumulation of the particle sizes is in the range of 3-7 µm, which also corresponds to the holes on the piezo vibrators.

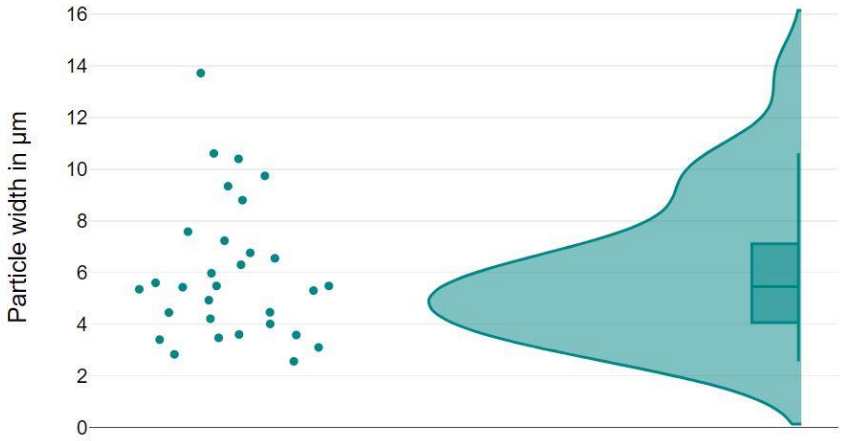

Figure 8f. Raincloud diagram based on microscope measurement data of the fog particles – most are in the range of 3 to 7 micrometres with a maximum around 5 micrometres

3.2. Observing of the Fog Layering and Fogging Behaviour in the Chamber

The behaviour of fog stratification is known and therefore also circulating fans have been used to prevent this phenomenon. The experiments carried out in advance show the situation very well. Figure 9a shows the interior of the fog chamber through the viewing window at the chamber entrance with the view to the exit window at light detector side.

Figure 9a. View from front to back inside the closed chamber with plastic lid without fog

In the first case, the chamber is filled with fog (Figure 9b) but without using the ten circulating fans. Hence, fog stratification begins due to the earth's gravitational pull and the fog particles begin to sink, which is clearly visible (Figure 9c).

Figures 9b, 9c. The fog in the chamber shows stratification without fans, and a sinking fog front after some time

In the second case, under the same conditions but with the circulating system switched on, it is visible that no layering takes place (Figures 9d, 9e).

Figures 9d, 9e. The fog in the chamber shows no stratification after some time with circulation

4. Testing and Characterization of the Operational Fog Chamber

In a next step, the assembled fog chamber is tested with a red laser beam, passing through the chamber filled with fog (Figures 10a, 10b, 10c). Particularly, it is interesting to address the question, whether there is any substantial difference between (i) using steam (hot fog) or ultrasonically generated (cold) fog, (ii) operating the chamber with or without ventilation system, and (iii) including an anti-condensation concept like the automatic glass-wiper system.

The performance of the fog chamber is evaluated based on the optical transmission through the chamber, recorded with the laser and detector system. The power at the detector is recorded over time. The signal strength varies depending on the fog density in the chamber. At the beginning of the measurement, the fog is very dense, and no light reaches the detector. After some time, the power signal rises again, as the fog dissipates.

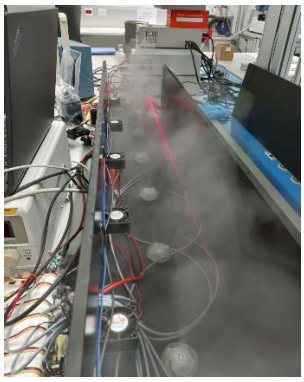

Figure 10a. Picture of the opened chamber with running fog sprayer system and laser beam

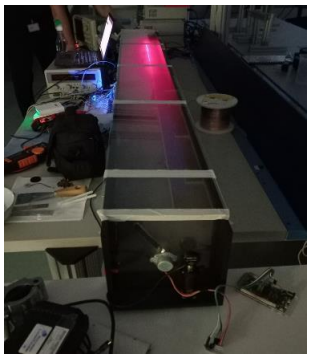

Figure 10b. Picture of the closed chamber with sealed glass panes and filled with fog

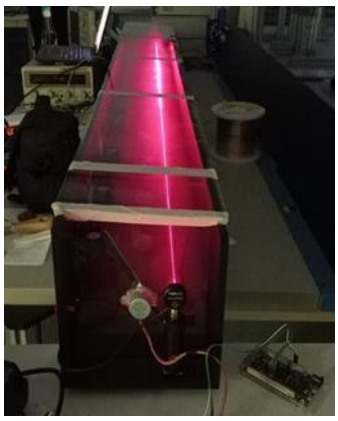

Figure 10c. Picture of the closed chamber after the fog has cleared and the laser reached the detector

5. Results

Following graphs, showing the transmittance through the fog chamber for different conditions, are displayed side by side. The left graphs (labelled "a") represent the measurements for the ultrasonic nebulizer fog, while the right graphs (labelled "b") show the measurements for the hot steam fog case. The diagram displays the detected light power of the laser, shown on the Y-axis, whereby the X-axis represents the timeline. At the beginning of the measurement, the fog source is switched on and the chamber is filled with fog for a few seconds until the source is switched off again. In this time, the power signal of the laser is lowest, because no light can reach the detector. After some time, the power signal rises again, when the fog dissipates.

In the first experiment, no wipers and no ventilation were used. Therefore, stratification and condensation occurred.

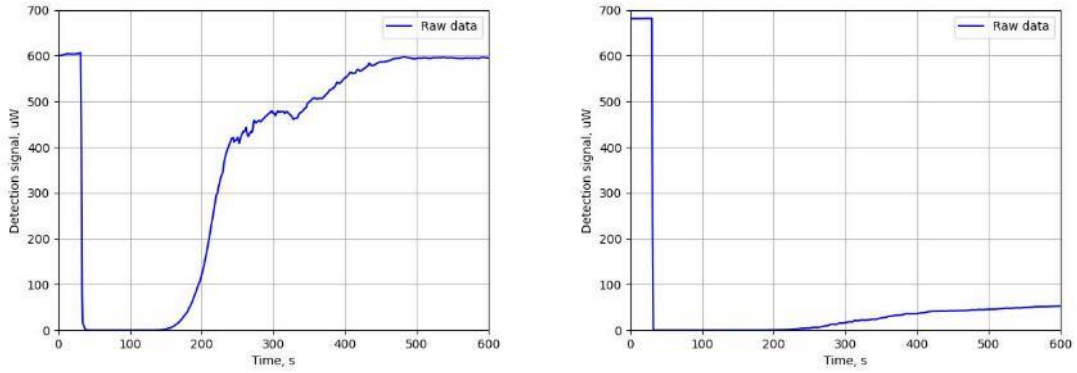

Figures 11a, 11b. Graph of the transmission detector signal before, meanwhile and after fog filling of the chamber for a) the piezo type and b) the steam cleaner with no treatment like wipers or ventilation

Figure 11a shows that the transmission for the piezo generated fog, whereas Figure 11b shows the hot steam fog (Figure 11b). Fog generated by the two sources behaves very differently. Particularly, the transmission signal for the hot steam fog is much smaller than in the case of piezo-generated fog and does not recover the initial value even after many minutes. The behaviour can be explained by a massive amount of condensation at the optical windows. Indeed, by activating the windscreen wiper system, an improvement could be observed, mainly for the hot steam fog (Figure12b). Due to the fact that the windscreen wiper is frequently blocking the laser beam, the raw data (blue curve) needed to be filtered and replotted (red curve). The filter is an easy function eliminating the frequent power jumps by only considering the maximum power values.

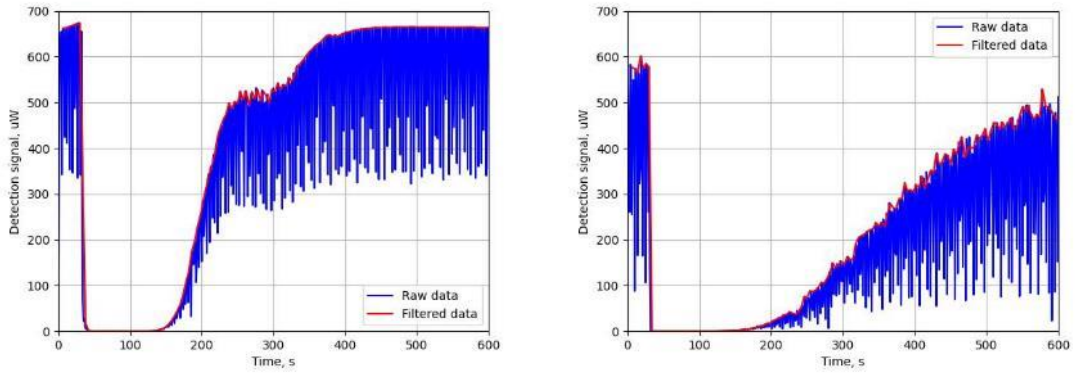

Figures 12a, 12b. Graph of the transmission detector signal before, meanwhile and after fog filling of the chamber for a) the piezo type and b) the steam cleaner with treatment of wipers but no ventilation

By activating the additional circulation system, a further improvement could be reached, which is clearly visible in Figure pair 13a and 13b. The plateau in the transmission observed in Figs. 11a and 12a in the time interval between 220s to 320s disappears (Figure 13a) by activating the fans, hinting that the effect is caused by stratification of the fog.

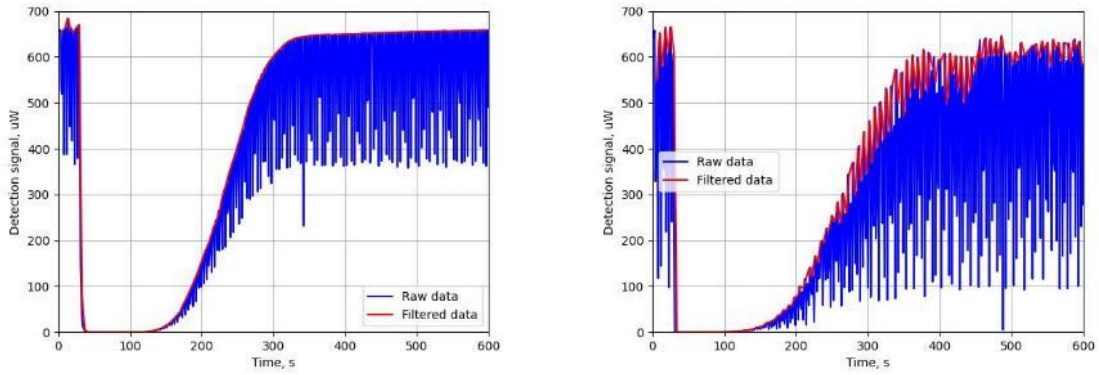

Figures 13a, 13b. Graph of the transmission detector signal before, meanwhile and after fog filling of the chamber for a) the piezo and b) the steam cleaner with treatment of wipers and ventilation

Figure 13a shows that by using a ventilating system, stratification is eliminated. Figure 13b shows that the combination of ventilation and windscreen wiping allows to recover a similar transmission behaviour for hot-steam and cold fog. Nevertheless, the cold fog generated by the ultrasonic transducer is more stable and performed better in the experiments, which is seen in the data.

6. Discussion

In the preliminary experiments with the two types of fog (ultrasonic nebulizers and hot steam), it was observed that the hot steam fog produced significantly more moisture and encountered more issues due to increased condensation compared to the ultrasonic nebulizers. Conversely, the ultrasonic nebulizers demonstrated minimal improvement from the wiper system, as there was almost unnoticeable condensation generated on the interior surfaces and windows of the fog chamber. However, the ultrasonic nebulizers with the cold fog were more prone to fog stratification, which could only be mitigated through the implementation of a ventilation system. The fog stratification can be seen in Figures 11a and 12a in the time interval 220s –

320s, when the curve showed a kinked and bended behaviour, which disappears when adding the ventilation system (Figure 13a). This issue of fog stratification was not observed with the hot steam fog, where the dynamics and circulation generated by the hot steam itself facilitated adequate mixing. However, even when the circulation system was activated, the hot steam fog maintained its own dynamics, resulting in larger fluctuations of the optical signals as compared to the cold fog. The practical implications of using ultrasonic nebulizers versus hot steam are, on the one hand, fewer problems with condensation and are more like natural fog, because it is also cold. On the other hand, producing fog with ultrasonic nebulizers, requires several units in series, which requires their own setups, whereas hot steam is available directly from commercial products and can be filled directly into a chamber.

The chamber presented in this work can be thought as modular. It can be made arbitrarily longer to investigate longer optical paths in the fog. Additionally, the cross-section of the chamber can be enlarged by adding at least a second identical module to the side to enable investigation of larger fields of view.

7. Conclusions

In conclusion, we presented the design and characterization of a laboratory fog-chamber. We compared the optical quality of the generated fog based on optical transmission measurements and we showed that cold fog generated by piezo nebulizers is more homogeneous and stable than fog generated by hot-steam sources. We also demonstrated the necessity to ensure an adequate ventilation system to prevent fog stratification, and an adequate system to remove condensation at the optical windows. The fog chamber showed here, does not aim at replacing large-scale meteorological testing facilities; it represents rather a step forward towards small laboratory-based meteorological test-stations. Being compact, affordable and modular, it is a practical tool that can foster the development of LIDAR systems and allow collecting a large amount of data for many different fog conditions, which is necessary for the development of AI-based image- and situation-recognition software. The modular design is particularly advantageous if someone needs a larger chamber or more fog. Then all one must do is build the chamber accordingly and expand it with fog systems. The chamber is also not limited to LIDAR sensors, all other optical sensors like ambient light sensors or laser detectors can be analysed.

Acknowledgment

This work has been jointly supported by the BMK (Austrian Federal Ministry for Climate Action, Environment, Energy, Mobility, Innovation and Technology) within the program “ICT of the future” under grant agreement no. 878713 (iLIDS4SAM-Project) and by Silicon Austria Labs (SAL), owned by the Republic of Austria, the Styrian Business Promotion Agency (SFG), the federal state of Carinthia, the Upper Austrian Research (UAR), and the Austrian Association for the Electric and Electronics Industry (FEEI).

References

Ballesta-Garcia, M., Peña-Gutiérrez, S., Val-Martí, A., & Royo, S. (2021). Polarimetric Imaging vs. Conventional Imaging: Evaluation of Image Contrast in Fog. *Atmosphere, 12*(7), 813. https://doi.org/10.3390/atmos12070813

Duthon, P., Colomb, M., & Bernardin, F. (2020). FOG classification by their droplet size distributions: application to the characterization of Cerema’s platform. *Atmosphere, 11*(6), 596. https://doi.org/10.3390/atmos11060596

Hahner, M., Sakaridis, C., Dai, D., & Luc, V. G. (2021). Fog simulation on real LiDAR point clouds for 3D object detection in adverse weather. *arXiv* (Cornell University). https://doi.org/10.1109/ICCV48922.2021.01500

Kooij, S., Astefanei, A., Corthals, G. L., & Bonn, D. (2019). Size distributions of droplets produced by ultrasonic nebulizers. *Scientific Reports, 9*(1). https://doi.org/10.1038/s41598-019-42599-8

Kutila, M., Pyykönen, P., Holzhüter, H., Colomb, M., & Duthon, P. (2018). Automotive LiDAR performance verification in fog and rain. *21st International Conference on Intelligent Transportation Systems (ITSC)*, 1695-1701. https://doi.org/10.1109/ITSC.2018.8569624

Linnhoff, C., Hofrichter, K., Elster, L., Rosenberger, P., & Winner, H. (2022). Measuring the influence of environmental conditions on automotive LIDAR sensors. *Sensors, 22*(14), 5266. https://doi.org/10.3390/s22145266

Liu, Q., Wu, B., Wang, Z., & Hao, T. (2020). Fog Droplet Size Distribution and the Interaction between Fog Droplets and Fine Particles during Dense Fog in Tianjin, China. *Atmosphere, 11*(3), 258. https://doi.org/10.3390/atmos11030258

Montalban, K., Reymann, C., Atchuthan, D., Dupouy, P., Riviere, N., & Lacroix, S. (2021). A Quantitative Analysis of Point Clouds from Automotive Lidars Exposed to Artificial Rain and Fog. *Atmosphere, 12*(6), 738. https://doi.org/10.3390/atmos12060738

Mothershed, D. M., Lugner, R., Afraj, S., Sequeira, G. J., Schneider, K., Brandmeier, T., & Soloiu, V. (2020). Comparison and evaluation of algorithms for LIDAR-Based contour estimation in integrated vehicle safety. *IEEE Transactions on Intelligent Transportation Systems, 23*(5), 3925–3942. https://doi.org/10.1109/tits.2020.3044753

Royo, S., & Ballesta-Garcia, M. (2019). An overview of LiDAR imaging systems for autonomous vehicles. *Applied Sciences, 9*(19), 4093. https://doi.org/10.3390/app9194093

Sawant, V., Meena, G., & Jadhav, D. (2012). Effect of negative air ions on fog and smoke. *Aerosol and Air Quality Research, 12*(5), 1007–1015. https://doi.org/10.4209/aaqr.2011.11.0214

Singh, V. P., Gupta, T., Tripathi, S. N., Jariwala, C., & Das, U. (2011). Experimental study of the effects of environmental and fog condensation nuclei parameters on the rate of fog formation and dissipation using a new laboratory scale fog generation facility. *Aerosol and Air Quality Research, 11*(2), 140–154. https://doi.org/10.4209/aaqr.2010.08.0071

Wu, J., Xu, H., Zheng, Y., & Tian, Z. (2018b). A novel method of vehicle-pedestrian near-crash identification with roadside LiDAR data. *Accident Analysis & Prevention, 121*, 238–249. https://doi.org/10.1016/j.aap.2018.09.001